Heliyon 10 (2024) e37897

Contents lists available at ScienceDirect

Heliyon

journal homepage: www.cell.com/heliyon

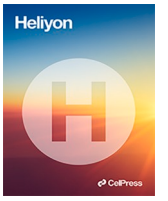

Research article

A novel proteomic prognostic signature characterizes the immune landscape and predicts nasopharyngeal carcinoma prognosis

Lixin Zhu [a], Wenliang Duan [a], Lijing Peng [a], Xinxin Shan [a], Yuan Liu [a], Zhenke Huang [a], Yunxiang Da [a], Yanyan Han [b,*]

[a] Department of Otolaryngology, Shanghai University of Medicine & Health Sciences Affiliated Zhoupu Hospital, Shanghai, 201318, China
[b] Department of Otolaryngology, Shanghai Punan Hospital, Shanghai, 200120, China

ARTICLE INFO

Keywords:
Nasopharyngeal carcinoma
Proteomics
Prognosis
RPscore
DUSP14

ABSTRACT

Background: Nasopharyngeal carcinoma (NPC) is a highly diverse and aggressive cancer type, leading to varying prognoses and responses to immunotherapy. This study aims to develop a protein-based signature that provides new insights into assessing the prognosis and immunotherapeutic response in NPC patients.

Methods and Results: We obtained transcriptomic and proteomic data for NPC from TCGA and CPTAC databases, respectively. Differentially expressed proteins with prognostic significance were identified using limma combined with uniCox analysis. A prognostic protein signature was created utilizing the LASSO algorithm. Receiver operating characteristic (ROC) curve analysis along with Kaplan-Meier survival analysis was conducted to assess the predictive accuracy of this signature. To evaluate immune infiltration levels among patients categorized by high or low risk scores (RPscores), we employed ssGSEA and ESTIMATE methods, while TIDE was used to forecast responses to immunotherapy. Our research pinpointed four critical prognostic proteins: CdSTA, AGR3, DUSP14, and LRRC17, allowing us to compute risk scores (RPscores). Kaplan-Meier curves demonstrated that individuals in the low-risk category exhibited better survival rates. Furthermore, RPscore effectively predicted overall survival across both training and testing cohorts. The ssGSEA results indicated that RPscore is linked with an immune-suppressive microenvironment correlating with diminished immune responses. Notably, DUSP14 showed significant upregulation in NPC cases; its role in promoting cell invasion and metastasis was confirmed through in vitro studies.

Conclusion: We have established a robust protein-related signature capable of accurately forecasting prognosis as well as immunotherapy outcomes for NPC patients. Moreover, DUSP14 emerged as a potential therapeutic target due to its strong association with patient prognosis in nasopharyngeal carcinoma.

1. Introduction

Nasopharyngeal carcinoma (NPC) is a squamous cell carcinoma that originates in the nasopharynx, particularly prevalent in East and Southeast Asia [1]. The outlook for individuals diagnosed with NPC remains unfavorable [2], even with notable progress in

* Corresponding author. Department of Otolaryngology, Shanghai Punan Hospital, Shanghai, China.
E-mail address: 405038500@qq.com (Y. Han).

https://doi.org/10.1016/j.heliyon.2024.e37897
Received 24 May 2024; Received in revised form 12 September 2024; Accepted 12 September 2024
Available online 18 September 2024

treatment options such as immunotherapy, chemotherapy, and radiation therapy in recent years. Currently, most patients are already in the advanced stage when diagnosed, with a high risk of recurrence and metastasis, and the 5-year survival rate is still only 40%–50 % [3]. Subsequently, it is crucial to identify valuable biomarkers that can offer therapeutic insights aimed at enhancing the prognosis for NPC patients [4].

NPC is believed to be assocaited with Epstein-Barr virus (EBV) infection, as well as, diet, smoking and genetic predisposition [5,6]. EBV infection creates a distinct immune microenvironment in NPC, leading to pronounced immune escape characteristics. EBV-infected nasopharyngeal carcinoma cells produce exosomes and cytokines that affect stromal cells' functions within the tumor [7]. Immune escape presents a significant challenge for the NPC's clinical management and treatment, particularly in the context of immunotherapy. The alteration of the tumor microenvironment is considered as a crucial mechanism of immune escape and is closely linked to metabolic processes. For example, chemotherapy has been shown to induce IL-18 secretion by macrophages. In tumor cells, it upregulates the LAT2 (amino acid transporter), which in turn upregulates CD47 expression and suppresses macrophages phagocytosis, facilitating tumor cell immune escape [8]. Additionally, HK2, a key glycolysis enzyme, phosphorylates IκBα, promoting its degradation and activating the NF-κB pathway. This activates PD-L1, contributing to tumor immune escape [9]. Therefore, a deeper understanding of metabolism-related proteins, especially secreted proteins, in shaping the tumor microenvironment and developing immunotherapy strategies is crucial for addressing tumor escape.

Recently, extensive proteomic studies have been employed to explore the properties of proteins, providing a thorough new understanding of disease mechanisms (including NPC), cellular metabolism, and various biological processes at the protein level [10,11]. However, there is a lack of studies focusing on the analysis of prognosis and prognostic markers in nasopharyngeal carcinoma based on protein expression levels.

The CPTAC project has generated extensive proteomic data for a wide range of tumors using mass spectrometry [12]. Leveraging CPTAC's proteomics data, we identified differently and prognostically relevant proteins in NPC and developed a prognostic model, termed RPscore, based on four key proteins using machine learning techniques. Our findings indicate that RPscore is associated with tumor grading and can distinguish the resistance to immunotherapy.

2. Materials and methods

2.1. Data collection

NPC proteomics datas were downloaded from CPTAC (https://portal.gdc.cancer.gov/), including normalized relative quantitative data from TMT labeling experiments in 105 NPC patients, along with matched clinical information such as age, sex, grade, and TMN stages. RNA-Seq data and clinical data of the 527 cases in The Cancer Genome Atlas Program (TCGA-HNSC) project were also collected. The RNA-Seq data matrix was normalized using TPM and subsequently log2 (x+1) transformed.

2.2. Difference and enrichment analysis

We screened proteins with a foldchange >1.3 and $P < 0.05$ using the 'limma' program (v3.50.3) [13], with adjustments made by the BH method. The analysis for biofunctional enrichment was conducted using the 'clusterProfiler' R package (version 4.2.2) and Sangerbox14,15 to perform Kyoto Encyclopedia of Genes and Genomes (KEGG) and Gene Ontology (GO) assessments. GO enrichment analysis was utilized to examine gene-related biological processes (BP), molecular functions (MF), and cellular components (CC), while KEGG analysis focused on investigating the signaling pathways associated with these genes [14,15]. A PPI network was constructed based on the String database (http://string-db.org/) [16]. We also conducted enrichment analysis of the PPI network using the Enrichr website (https://maayanlab.cloud/Enrichr/) [17]. The top 10 enrichment items and their p-values are visualized in bar charts, with bars colored according to their p-values.

2.3. Classification model construction and validation

Using the R package "glmnet", we conducted a least absolute shrinkage and selection operator (LASSO) Cox regression (v4.1-4) [18] to identify differential prognostic proteins in the data set for training, and calculate a risk protein score (RPscore) for each NPC case using the equation below. Differential proteins were analyzed using univariate Cox regression and Kaplan-Meier survival analysis to identify proteins that were significant in both prognostic methods, which were then used for LASSO modeling with the R package "glmnet". The training set and test set were constructed by split the samples randomly, and the LASSO model was trained on the training set to get a multi-protein risk score (RPscore), calculated as follows, where $coef_i$ represents the coefficient of protein P_i in the model:

$$RPscore = \sum_{i=1}^{n} coef_i * P_i$$

High and low-risk groups were identified by divided samples by the median RPscore as the cut-off [19]. To evaluate the accuracy of RPscore, receiver operating characteristic (ROC) curve analysis was performed across the training, test, and entire datasets. Kaplan-Meier curves were employed to examine the ability of the RPscore to predict prognosis of NPC patients.

2.4. Immune infiltration analysis

The immune cell infiltration profiles in the tumor microenvironment (TME) were assessed by the single sample gene set enrichment analysis (ssGSEA) [20]. Previous studies identified 23 immune cell types infiltrating the TME according to genomes data [21]. Estimation of Stromal and Immune cells in MAlignant Tumor tissues using Expression data (ESTIMATE) [22] algorithm was used to calculate the proportions of stromal and immune cells. Correlation heatmaps were generated by the R package "corrplot" (v0.92) to visualize the relationships between infiltrating immune cells.

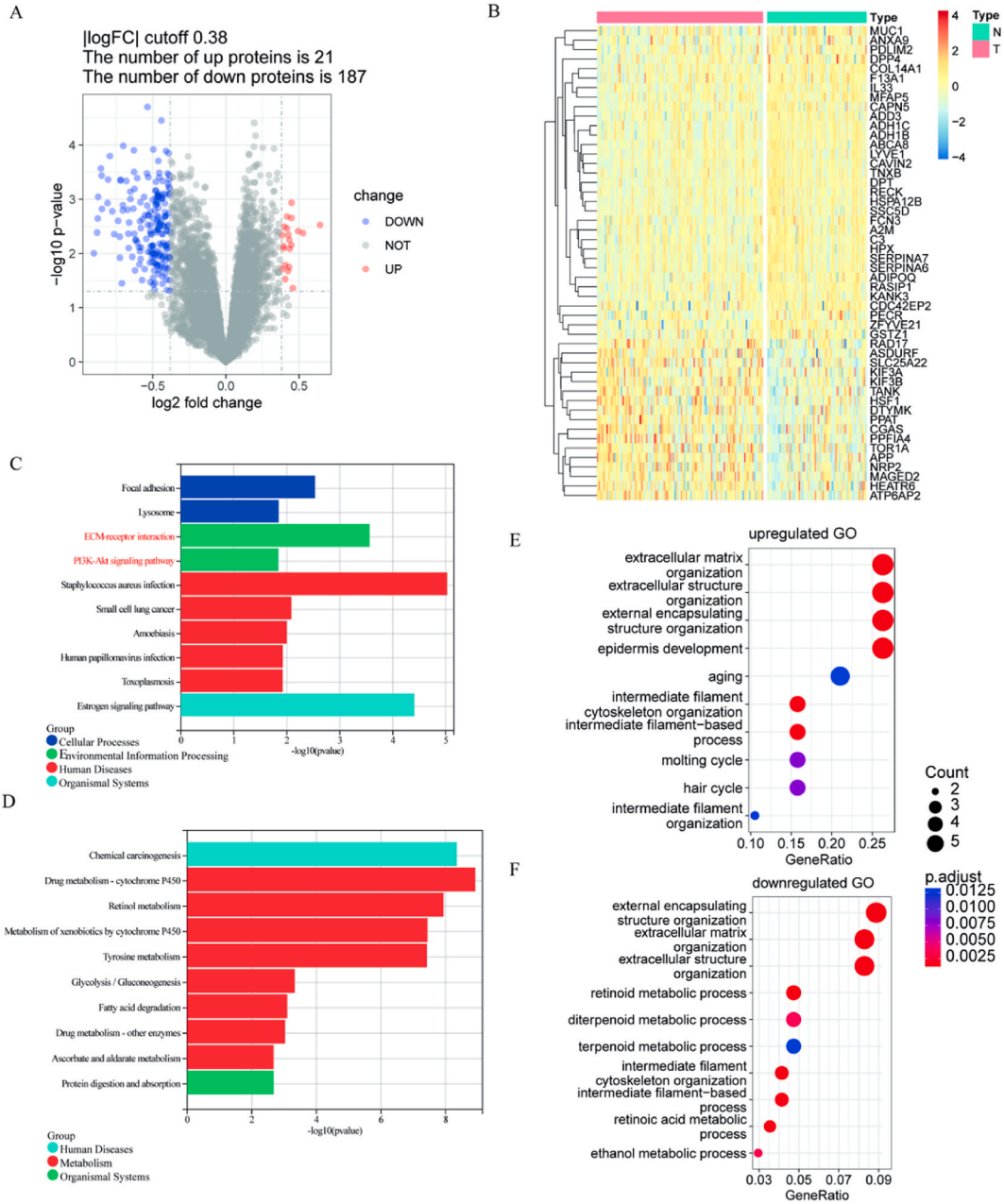

Fig. 1. Differential protein identification and functional analysis of NPC.
(A) Volcano map of differential proteins. (B) Heat map of Top 50 differential proteins. KEGG enrichment analysis of (C) up- and (D) down-regulated differential proteins. Go analysis of (E) up- and (F) down-regulated differential proteins.

2.5. Cell culture, transient transfection, RNA extraction and quantitative real-time PCR (qRT-PCR)

The human nasopharyngeal epithelial cell line NP69 and four nasopharyngeal carcinoma cell lines (HEN-1, HEN-2,5–8F, C666-1) were purchased from the Cell Institute of the Chinese Academy of Sciences for this study. All cells were cultured in DMEM (Gibco, USA) containing 10 % fetal bovine serum (Gibco, USA) or RPMI-1640 (Gibco, USA). Negative control (NC) and DUSP14 siRNA (Genomeditech, China) were transfected into nasopharyngeal carcinoma cells using Lipofectamine 2000 (Invitrogen, USA) according to the manufacturer's protocol. Cells were transfected with 30 pmol siRNA, incubated for 24 h, and subsequent experiments were conducted after confirming transfection efficiency via RT-qPCR [23].

Total mRNA was extracted from cultured cells and reverse transcribed into cDNA using a reverse transcription kit (Takara) according to the manufacturer's protocol. The cDNA was then incubated with SYBR Green incubation and amplified using a real-time PCR system. mRNA expression levels were normalized to GAPDH expression. The primer sequences for this study are shown in Table S1.

2.6. Wound healing and transwell assay

Wound healing and transwell assays were conducted to assess the migration and invasion capabilities of nasopharyngeal carcinoma cells following siRNA transfection. Cells (1.5×10^5) were seeded into the respective compartments and incubated for 48 h, following the manufacturer's protocol.

2.7. Statistical analysis

Kaplan-Meier curves with log-rank test were used to evaluate OS associated with differential proteins. Univariate and multivariate Cox regression analyses were conducted to assess the prognostic value of differential proteins and clinical factors. The correlation between RPscore and clinicopathological features was determined using the Wilcoxon or Kruskal-Wallis tests. Pearson correlation was performed to assess the relationship between immune cells and RPscore. Receiver operating characteristic (ROC) curves, generated using the 'survival ROC' package in R, along with the area under the curve (AUC), were used to assess the prognostic capability of overall survival (OS) risk scores at three years. The version of R employed for this analysis was 4.0.3. A p-value threshold of less than 0.05 was deemed statistically significant.

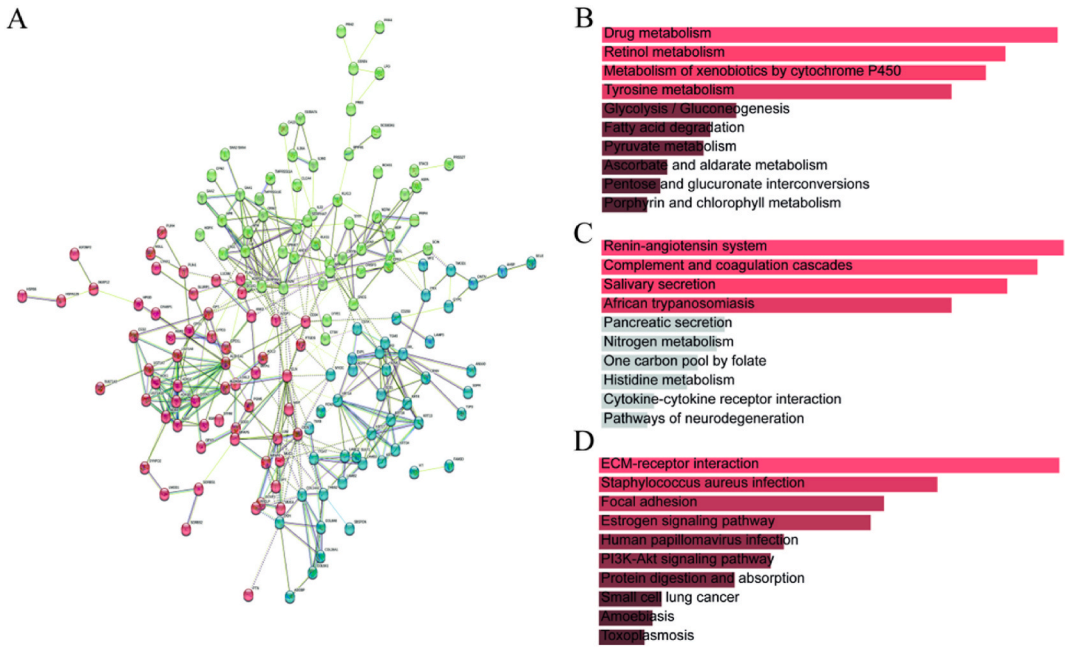

Fig. 2. Construction of protein-protein interaction network.
(A) PPI network clustering diagram generated by String program. Enrichment analysis results of (B) red, (C) green, (D) blue clusters. (For interpretation of the references to color in this figure legend, the reader is referred to the Web version of this article.)

3. Results

3.1. Analysis of differentially expressed genes in nasopharyngeal carcinoma and their functional implications

Differential analysis was conducted using the limma method, revealing 208 differently expressed (DE) proteins between 105 tumor samples and 63 normal samples. DE proteins included 21 up-regulated and 187 down-regulated ones (Fig. 1A). A heat map visualization of the most significant 50 DE proteins is shown in Fig. 1B. The differently expressed proteins were subjected to GO and KEGG analyses to elucidate functions and pathways of them. KEGG enrichment indicated that up-regulated proteins were closely associated with ECM-receptor interaction, the PI3K-Akt signaling pathway, and cancer pathways, while down-regulated proteins were predominantly associated with various drug metabolism pathways, such as cytochrome P450-mediated metabolism of xenobiotics (Fig. 1C and D). From the biological process category, it was observed that these proteins are primarily involved in extracellular structural organization and the extracellular matrix (Fig. 1E and F). This suggests that metabolic alterations is important for the progression of NPC disease. When comparing transcriptomics and proteomics data, among the 7771 proteins/mRNAs detected in both TCGA and CPTAC, only 175 protein-mRNA pairs were commonly significantly up/down regulated in the same direction (Fig. S2B). Functional analysis through GO enrichment of these 175 protein-mRNA pairs showed high consistency with the differential proteins identified (Figs. S2C–F).

3.2. PPI network reveals distinct clusters determining NPC disease characteristics

By importing the differential proteins into the STRING program and clustering them using the K-mean algorithm, 3 different clusters were identified within the protein-protein interaction (PPI) network (Fig. 2A). These clusters appear to represent different functional categories. Enrichment analysis of the red, green, and blue clusters, which contain 72, 78, and 55 proteins respectively, revealed the following functions: The red cluster is involved in drug metabolism functions, including Drug metabolism, Retinol metabolism, Metabolism of xenobiotics by cytochrome P450, and Tyrosine metabolism (Fig. 2B); The green cluster is associated with inflammatory and immune functions, such as Complement and coagulation cascades and cytokine-cytokine receptor interactions (Fig. 2C); The blue cluster relates to tumor aggressiveness, including ECM-receptor interaction, Focal adhesion, and the PI3K-Akt signaling pathway (Fig. 2D). These results suggest that the functional proteins in these clusters play a synergistic role in NPC progression. Details of the result of Enrichr analysis are provided in Table S2, including p-values and overlapped genes of each terms.

3.3. Construction of protein prognostic models

In the follow-up analysis, 208 proteins significantly associated with prognosis in NPC patients were included. First, five proteins

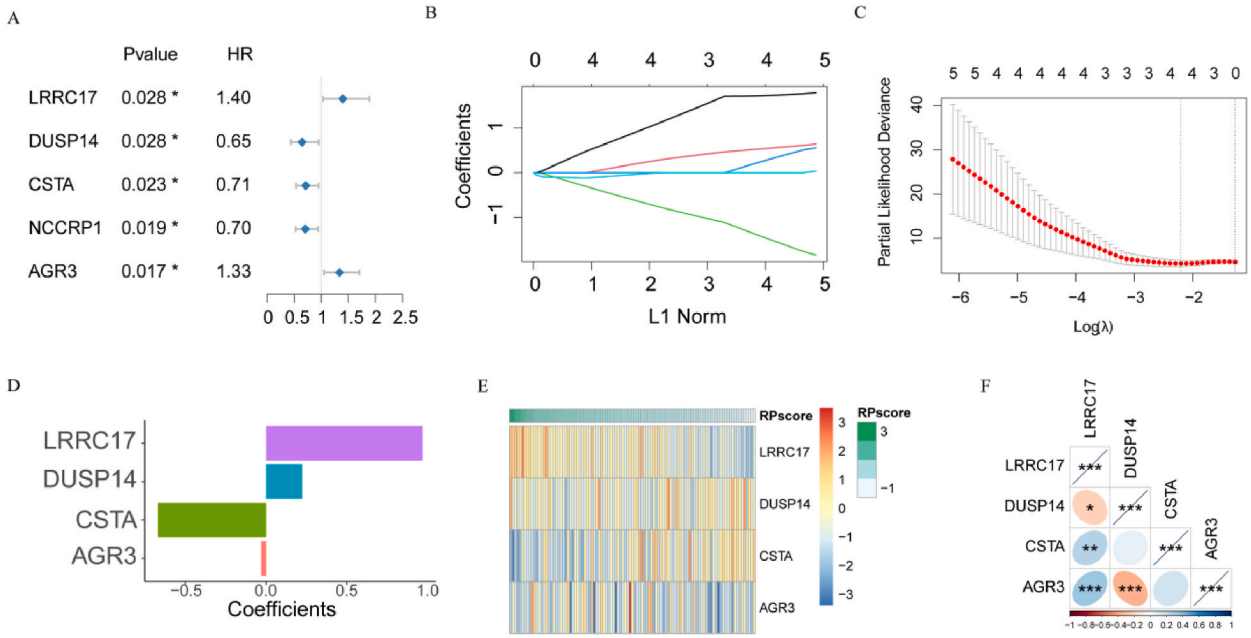

Fig. 3. Prognostic Model Construction.
(A) Forest plot of differential protein prognostic screening. (B–C) The lasso algorithm screens the optimal λ value and the number of proteins after corresponding constraints. (D) Coefficients for each protein in the model. (E) Expression of 4 proteins in high and low RPscore. (F) Correlation of 4 proteins.

were identified as being prognostically significant by filtering based on univariate Cox regression analysis (Fig. 3A). To determine the model accuracy, training set and a test set (n = 52 and 53, respectively) were established by randomly dividing 105 NPC patients into sets. Lasso regression analysis refined the molecules for the prognostic model, resulting in the identification of four key genes to construct the model specifically in the training set (Fig. 3B and C). The model coefficients are shown in Fig. 3D. Prognostic score for each patient was calculated based on the levels of these four proteins using the formula: RPscore = (0.968 × LRRC17 expression level) + (0.223 × DUSP14 expression level) + (−0.667 × CSTA expression level) + (−0.028 × AGR3 expression level). LRRC17 and AGR3 were more highly expressed in the high RPscore group, while DUSP14 and CSTA were more prevalent when RPscore was lower (Fig. 3E). Correlation analysis further demonstrated the relationships between these four proteins, with AGR3 having the highest negative correlation with DUSP14 ($R < -0.6$; $P < 0.05$) (Fig. 3F).

Since previous studies have indicated that the mRNA-protein concordance is only about 50 % [24], we compared transcriptome data of the TCGA-HNSC cohort with protein data from CPTAC. Compared to normal tissues, in tumors, CSTA and AGR3 were downregulated at both RNA and protein levels, while DUSP14 was upregulated at both levels. However, LRRC17 showed no differential expression at therth mRNA level, but its protein levels were decreased significantly (all $p < 0.05$) (Figs. S3A–B). Fu ermore, among the mRNAs, only CSTA was associated with NPC prognosis. (Fig. S3C). These results suggest that revealing the prognostic features of NPC requires both protein and RNA data, as relying solely on protein data is insufficient.

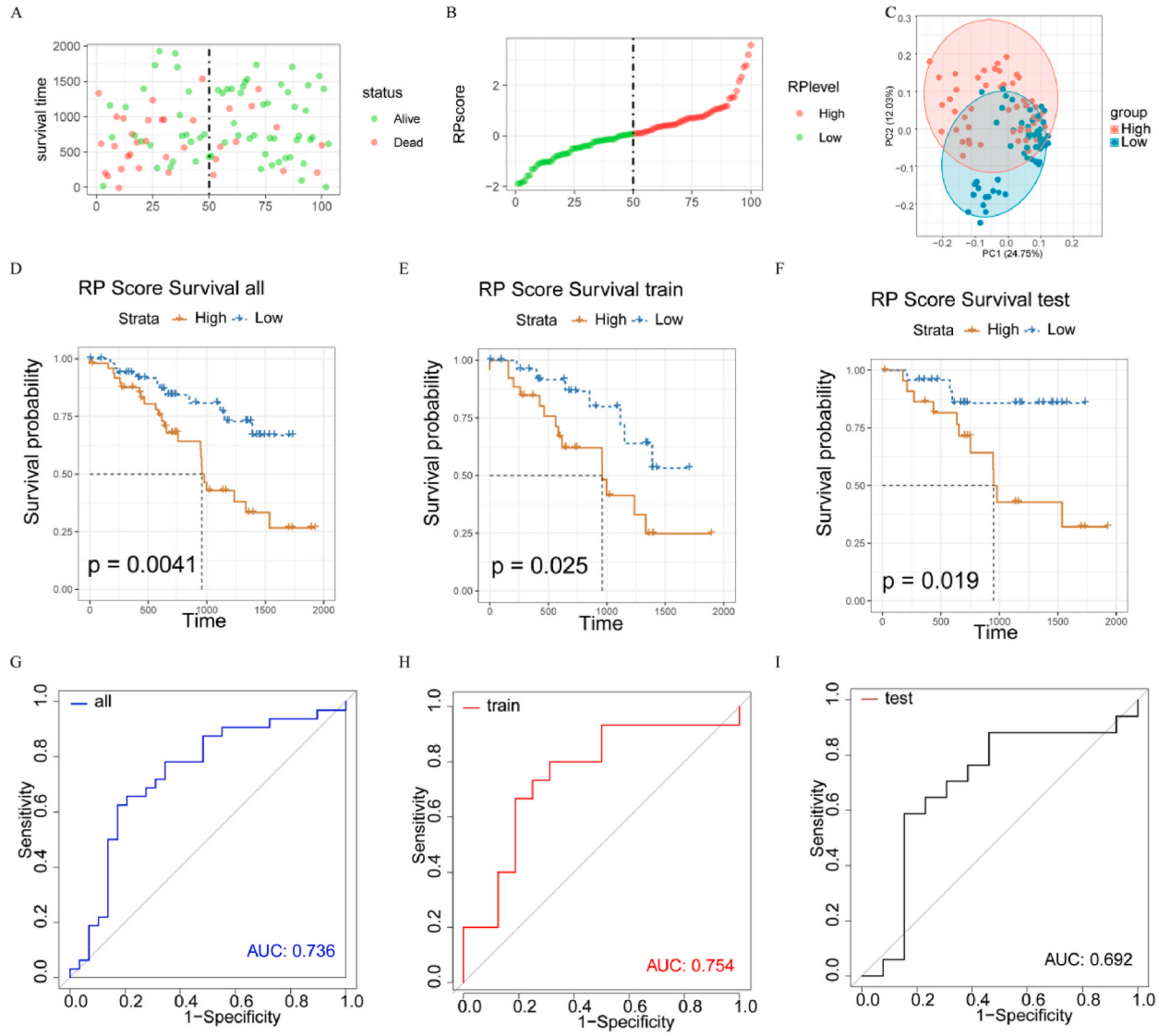

Fig. 4. Validation of the prognostic model.
(A) Distribution of survival status between high and low RPscore. (B) Sort by RPscore from low to high. (C) PCA distribution map of high and low RPscore. Kaplan-Meier survival curve plot for (D) all NPC patients, (E) training set and (F) test set. ROC curves for (G) all NPC patients, (H) training set and (I) test set.

3.4. Robustness of RPscore in NPC prediction

Scatter plots of RPscore distribution and median values indicated that patients with higher RPscore had higher mortality rates (Fig. 4A and B). PCA plot showed that patients with higher and lower RPscore were distributed in distinct orientations, confirming the reliability of the classification (Fig. 4C). Kaplan-Meier survival curves for all NPC patients, as well as for the training and test sets separately, demonstrated that high-RPscore patients had poorer prognosis in each cohort (all $p < 0.05$) (Fig. 4D–F). AUC values for the total NPC cohort, training set, and test set were 0.736, 0.754, and 0.692, respectively (Fig. 4G–I). Therefore, RPscore exhibits high accuracy and stability in predicting NPC patients prognosis.

3.5. High RPscore represents higher histological grading of NPC patients

We compared RPscore with various clinical characteristics and found no correlation between RPscore and age, gender, TN, and stage of NPC patients (Fig. 5A–D, F). In contrast, patients with higher histological grades (G2-3) had a significantly higher RPscore (Fig. 5E) compared to those with lower grades (G1). Univariate Cox analysis showed that only histological grade and RPscore were associated with NPC prognosis ($p < 0.05$; Fig. 5G), while multivariate Cox analysis further confirmed that RPscore and histological grade were independent prognostic factors for NPC patients ($p < 0.05$; Fig. 5H). This explains why RPscore did not correlate with other pathological factors.

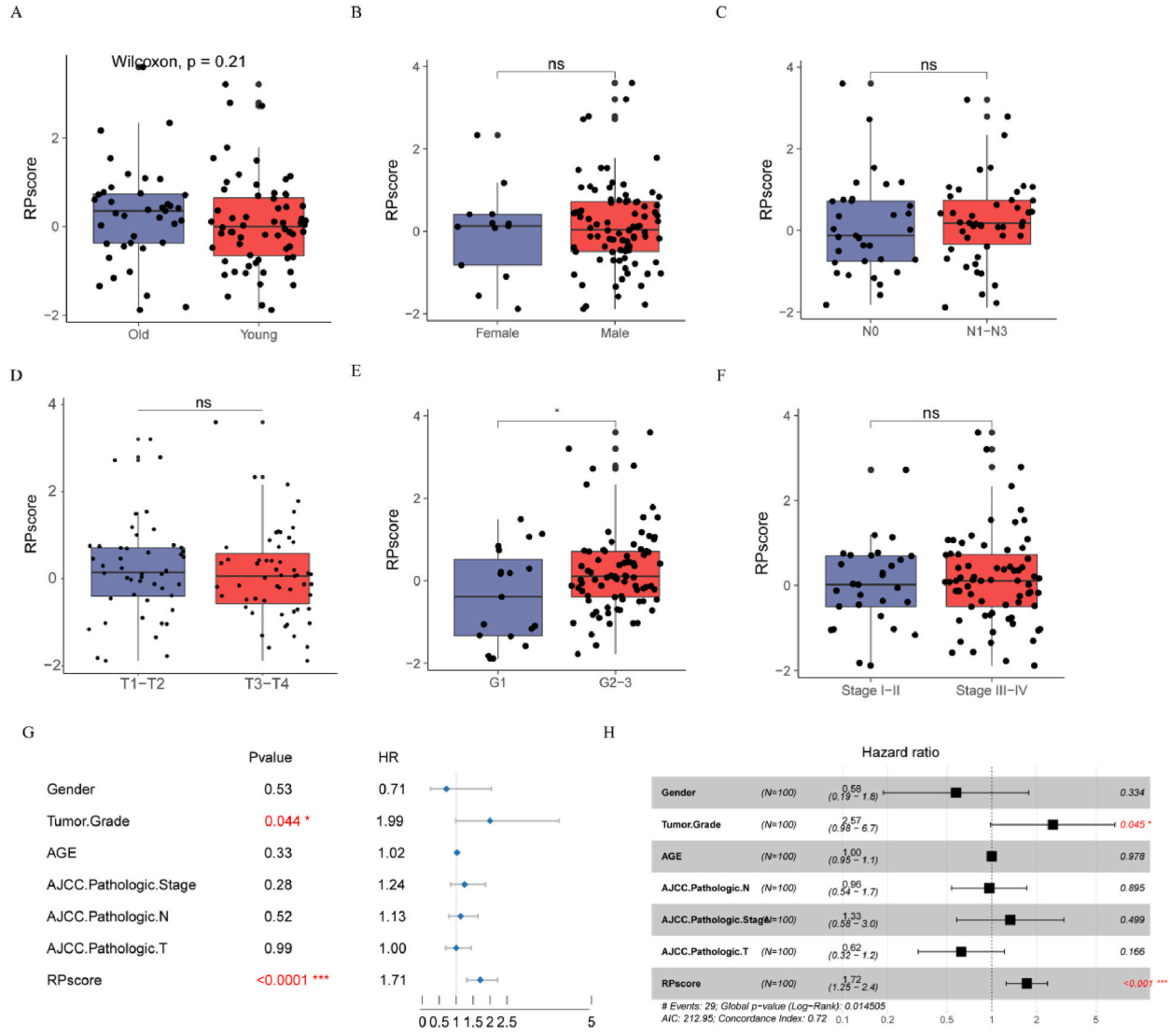

Fig. 5. Relationship between RPscore and clinical characteristics, including (A) age, (B) gender, (C) N stage, (D) T stage, (E) Grade, (F) Stage. (G) Univariate and (H) multivariate cox analysis of clinical characteristics and RPscore.

3.6. RPscore can be characterized as an immunosuppressive feature of NPC

Tumor immune cell infiltration is widely recognized as a crucial immune features of TME. Our previous findings suggest that differential proteins may be associated with cellular response. So we wanted to know whether there is a relationship between RPsocre and immune cell infiltration. Different types of immune cells are involved in anti-tumor responses and tumor immune escape processes, with tumor growth, invasion, and metastasis being closely linked to immune cells. Additionally, stromal cells are thought to significantly influence tumor growth, disease progression, and drug resistance [6,25]. The ESTIMATE result suggested that high-RPscore patients had higher immune, stromal and ESIMATE scores, indicating a higher level of immune escape (Fig. 6A–C). To explore the distribution and correlation of tumor-infiltrating immune cells in the CPTAC cohort, we assessed the level of infiltration of 23 immune cell types in each sample using ssGSEA (Fig. 6D), EPIC (Fig. S4), CIBERSORT [26] (Fig. S5), and MCP-Counter [27] (Fig. S6). The high-RPscore group exhibited higher abundance of immunosuppressive cells, such as macrophages, MDSC, and Tregs ($p < 0.05$) (Fig. 6D). A similar trend was observed for T follicular helper cells in the CIBERSORT results (Fig. S4). Correlation analysis further revealed that, while there was no correlation with MDSC (Fig. 6G), RPscore was positively correlated with macrophages and Tregs (Fig. 6E and F). Higher levels of immunosuppression in patients with a high RPscore may contribute to increased tumor escape. Consequently, RPscore patients were further evaluated using the TIDE algorithm (Fig. 6H), which showed a positive correlation between RPscore and T-cell dysfunction (Fig. 6I).

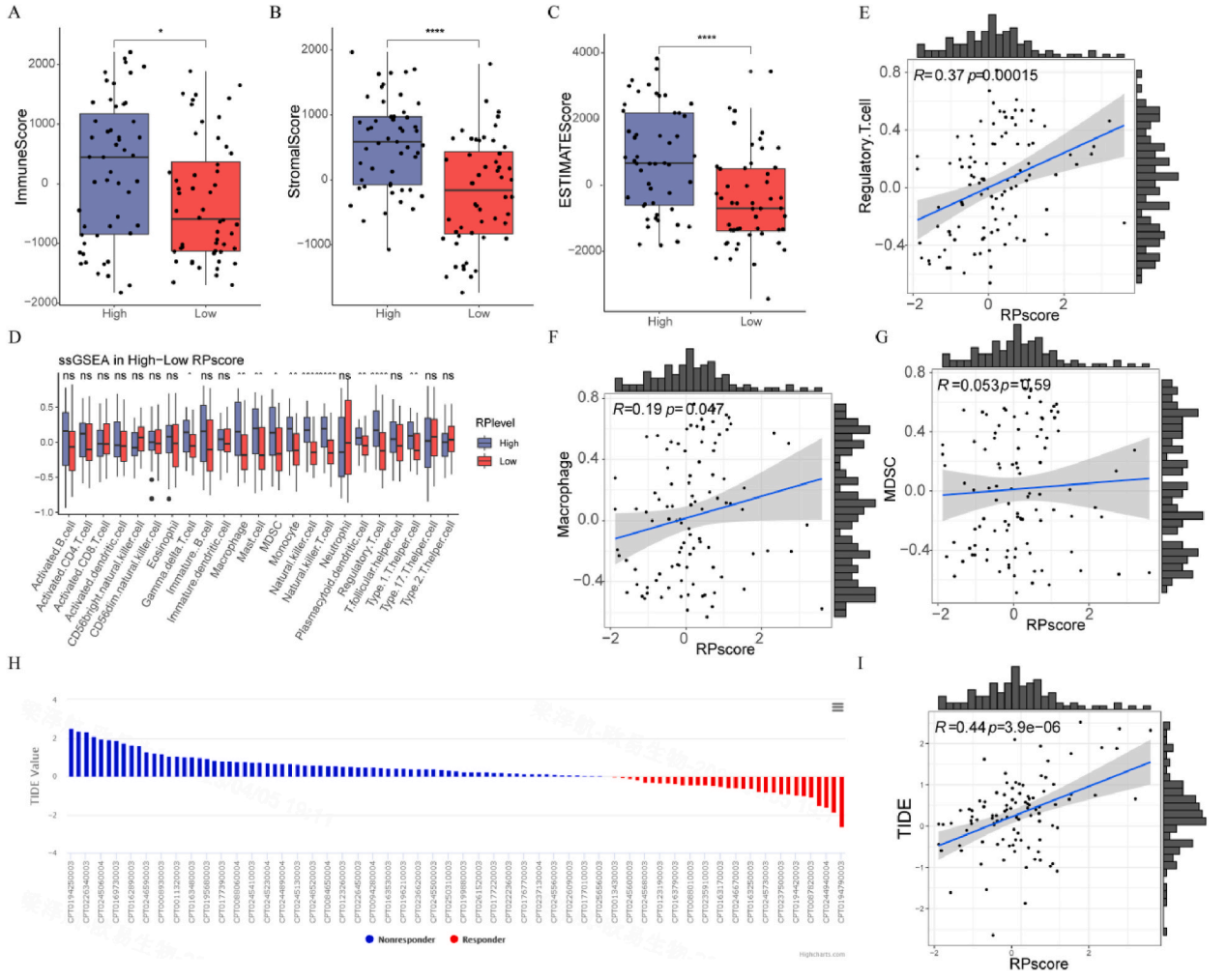

Fig. 6. Correlation analysis between RPscore and immune cell infiltration.
Correlation between RPscore and (A) immune score, (B) matrix score and (C) ESTIMATE score. (D) The ssGSEA algorithm calculates the relative abundance of RPscore and 23 immune cell subsets. Correlation of (E) macrophages, (F) Tregs and (G) MDSCs with RPscore. (H) TIDE scoring value of NPC patients. (I) Correlation between TIDE scoring value and RPscore.

3.7. DUSP14 is upregulated in NPC cells and promotes migration and invasion in vitro

DUSP14 expression in NPC cells, compared to normal human nasopharyngeal epithelial cell lines, was assessed and significantly upregulated in all four NPC cell lines ($P < 0.05$; Fig. 7A). DUSP14 was knocked down in HEN2 and HEN1 cells in vitro (Fig. 7B and C). The Transwell assay (migration assay) demonstrated that depletion of DUSP14 reduced migration ability ($P < 0.05$; Fig. 7D). Similarly, wound healing assay showed that knockdown of DUSP14 inhibited cell migration ability ($P < 0.05$; Fig. 7E and F).

4. Discussion

To some extent, the proteome provides more meaningful insights than the transcriptome. Unlike RNA expression, protein expression reflects the outcomes of post-transcriptional modifications, alternative splicing, and ribosome activity. Proteins are primary carriers of biological functions. Our results also confirm that there is not always a direct correspondence between the transcriptome and proteome, validating the importance of proteome-based prognostic studies. Using CPTAC proteomic data, a prognostic model was developed that includes four essential proteins and can effectively predict the survival of patients with NPC. In addition, we found that RPscore was positively correlated with histological grading and represented an immunosuppressive feature of NPC.

Differently expressed proteins in NPC are enriched in several key pathways, which can be broadly categorized into metabolism, immunity, and tumor malignant progression. We identified ECM [28]-receptor interaction pathway as a major pathway involved in the dysregulation of proteins in NPC. Early research highlights the role for ECM degradation in cancer metastasis. Serglycin, a proteoglycan component of the ECM, serving as an independent unfavorable prognostic indicator, is known to promote NPC metastasis [29]. In renal cell carcinoma, the activation of the GSK3β pathway by acylglycerol kinase promotes tumor growth and metastasis through the enhancement of PI3K/AKT signaling [30]. Additionally, miR-3188 regulates NPC proliferation and chemosensitivity through a positive feedback loop involving FOXO1 and the mTOR-p-PI3K/AKT -c- JUN signaling pathway [31]. Thus, protein interactions within the blue cluster are crucial in regulating NPC malignancy. Furthermore, glycolysis/gluconeogenesis is a well-established aspect of tumor metabolic reprogramming [32]. Our findings also associate tyrosine metabolism, fatty acid degradation, and pyruvate metabolism with NPC. Previous research had revealed tyrosine kinase is associated with cell motility and disease progression in head and neck squamous cell carcinoma [33]. Fatty acid oxidation can facilitate NPC cell proliferation through nucleoside metabolism [34], and targeting CPT1A-mediated fatty acid oxidation can enhances NPC sensitivity to radiotherapy [35]. According to these results, targeting metabolic pathways is a new potential strategy for NPC treatment.

Here we constructed a multi-protein model using CPTAC data by screening for differently expressed and prognostic-related proteins and performing LASSO regression analysis. This model identified independent prognostic factors for NPC and classified patients into two prognostic subgroups based on the RPscore. Kaplan-Meier curves, ROC curves, and PCA downscaled plots were used to

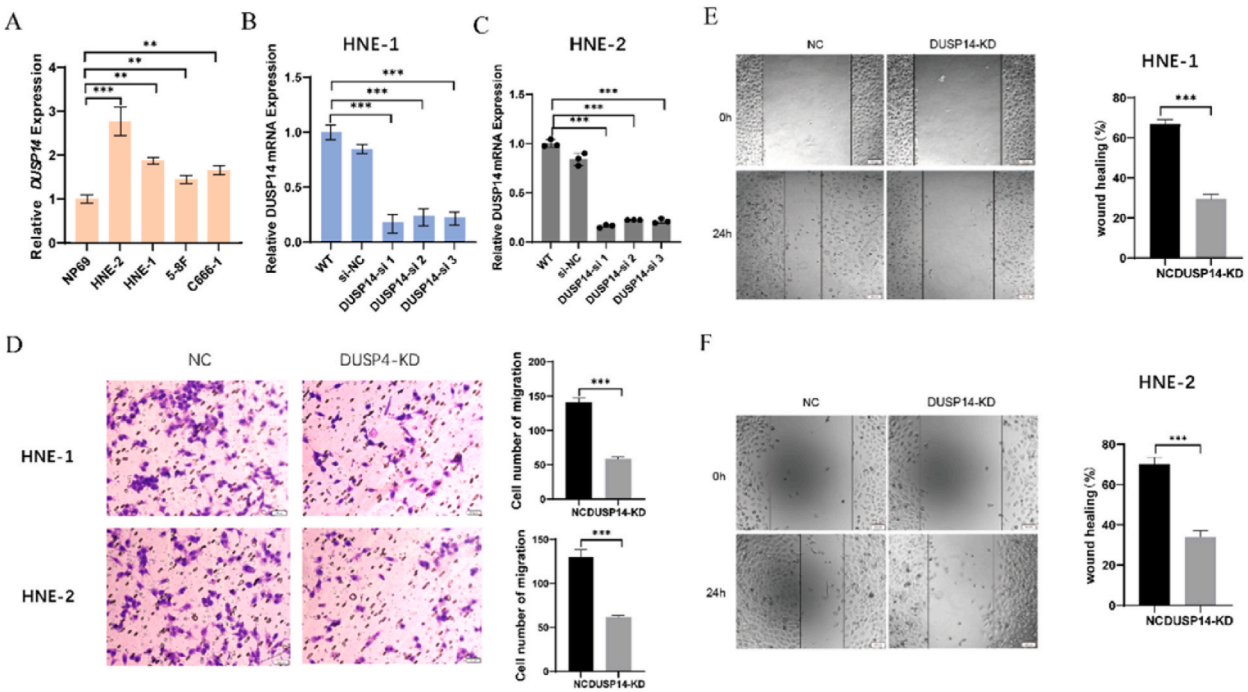

Fig. 7. DUSP14 is upregulated in NPC cells and promotes migration and invasion in vitro. (A) DUSP14 expression in normal nasopharyngeal epithelial cells and NPC cells. DUSP14 is knocked down in (B) HEN1 and (C) HEN2 cells. (D) Quantitative analysis of migrating NPC cell numbers. (E–F) Quantitative analysis of wound closure.

demonstrate that RPscore has superior predictive performance. A key finding is that RPscore can be used as an immunosuppressive marker for NPC. Immune cells are crucial for the response of immunotherapy as they are the cellular basis of it. Understanding the TME is essential for revealing of molecular mechanisms and developing new immunotherapeutic strategies [36]. In our study, immune cell infiltration were analyzed by various methods, with ssGSEA results considered the most reliable due to its applicability across different expression matrices. Other methods, based on mRNA expression, showed varying results. For T-regulatory cells, some consistency was observed across different algorithms. Macrophages were found to be more prevalent in patients with high RPscore, which may represent a poorer prognosis. This is because NPC exosomes can induce macrophages to produce IL-6, thereby promoting tumorigenesis [37]. In addition, MDSC has been shown to induce a pro-metastatic tumor microenvironment [38] and lead to resistance against nasopharyngeal carcinoma to overt T-cell therapies [39]. The cytotoxic T cells did not show significant differences across RPscore levels, suggesting that their cytotoxicity and cell killing are not directly related to RPscore. However, the changes observed in Tregs suggest that T cell ancillary roles in antigen presentation and signaling are significant in both high and low RPscore NPC samples. EBV-EBNA1 contributes to an immunosuppressive microenvironment in NPC, because it facilitates chemotaxis of regulatory T cells [40]. Therefore, the high expression of suppressive immune cells in patients with high RPscore creates an immunosuppressive microenvironment that facilitates tumor escape and results in poor prognosis.

Dual-specificity phosphatases (DUSPs) are capable of dephosphorylating both phosphotyrosine and phosphoserine/threonine residues on the same substrate, thus influencing a range of cellular functions [41]. Research had revealed that DUSP14 is important in pancreatic cancer, where it influences proliferation, invasion, and metastasis via modulating EMT, resulting in a deteriorate survival profile [42]. Our findings confirm that DUSP14 is upregulated in NPC. Furthermore, knockdown of DUSP14 effectively reduced both proliferation and migration of NPC cells.

However, there are limitations associated with research based on statistical analysis. Sample bias is an unavoidable factor, especially when data are drawn from various sources and sequencing methods. Results from statistical analyses may reflect mere correlation rather than direct causal relationships. For clinical application, further validations in larger cohorts and additional experimentations are necessary.

5. Conclusion

In summary, this study introduces a novel prognostic marker for NPC based on proteomic data. Additionally, the relationship between this prognostic marker and clinical characteristics was investigated, along with its connection to the tumor microenvironment. The present study provides a valuable theoretical insights into the mechanism underlying NPC development and identifies potential therapeutic targets.

Ethics approval and participation consent

This study did not involve any animal testing or human samples, thus ethics approval was not necessary.

Consent for publication

Not applicable.

Data availability statement

The data supporting the results of this research can be obtained from the corresponding author, [YH], upon reasonable request.

Funding information

This work received support from the People's Livelihood Research Special Medical and Health Project funded by the Shanghai Pudong New Area Science and Technology Development Fund Institution (Grant No. PKJ2022-Y101).

CRediT authorship contribution statement

Lixin Zhu: Writing – original draft. **Wenliang Duan:** Data curation. **Lijing Peng:** Formal analysis. **Xinxin Shan:** Supervision. **Yuan Liu:** Resources. **Zhenke Huang:** Software. **Yunxiang Da:** Conceptualization. **Yanyan Han:** Conceptualization.

Declaration of competing interest

The authors declare that they have no known competing financial interests or personal relationships that could have appeared to influence the work reported in this paper.

Acknowledgments

Not applicable.

Appendix A. Supplementary data

Supplementary data to this article can be found online at https://doi.org/10.1016/j.heliyon.2024.e37897.

References

[1] F. Bray, J. Ferlay, I. Soerjomataram, R.L. Siegel, L.A. Torre, A. Jemal, Global cancer statistics 2018: GLOBOCAN estimates of incidence and mortality worldwide for 36 cancers in 185 countries, Ca - Cancer J. Clin. 68 (6) (2018) 394–424, https://doi.org/10.3322/caac.21492.

[2] Y. Bensouda, W. Kaikani, N. Ahbeddou, R. Rahhali, M. Jabri, H. Mrabti, H. Boussen, H. Errihani, Treatment for metastatic nasopharyngeal carcinoma, Eur Ann Otorhinolaryngol Head Neck Dis 128 (2) (2011) 79–85, https://doi.org/10.1016/j.anorl.2010.10.003.

[3] J.D. Cramer, B. Burtness, R.L. Ferris, Immunotherapy for head and neck cancer: recent advances and future directions, Oral Oncol. 99 (2019) 104460, https://doi.org/10.1016/j.oraloncology.2019.104460.

[4] J. Zhang, Y. Li, J. Zou, C.T. Lai, T. Zeng, J. Peng, W.D. Zou, B. Cao, D. Liu, L.Y. Zhu, et al., Comprehensive analysis of the glutathione S-transferase Mu (GSTM) gene family in ovarian cancer identifies prognostic and expression significance, Front. Oncol. 12 (2022) 968547, https://doi.org/10.3389/fonc.2022.968547.

[5] L.L. Tang, Y.P. Chen, C.B. Chen, M.Y. Chen, N.Y. Chen, X.Z. Chen, X.J. Du, W.F. Fang, M. Feng, J. Gao, et al., The Chinese Society of Clinical Oncology (CSCO) clinical guidelines for the diagnosis and treatment of nasopharyngeal carcinoma, Cancer Commun. 41 (11) (2021) 1195–1227, https://doi.org/10.1002/cac2.12218.

[6] H. Chi, X. Xie, Y. Yan, G. Peng, D.F. Strohmer, G. Lai, S. Zhao, Z. Xia, G. Tian, Natural killer cell-related prognosis signature characterizes immune landscape and predicts prognosis of HNSCC, Front. Immunol. 13 (2022), https://doi.org/10.3389/fimmu.2022.1018685. Original Research.

[7] H. Huang, S. Li, Q. Tang, G. Zhu, Metabolic reprogramming and immune evasion in nasopharyngeal carcinoma, Front. Immunol. 12 (2021) 680955, https://doi.org/10.3389/fimmu.2021.680955.

[8] Z. Wang, B. Li, S. Li, W. Lin, Z. Wang, S. Wang, W. Chen, W. Shi, T. Chen, H. Zhou, et al., Metabolic control of CD47 expression through LAT2-mediated amino acid uptake promotes tumor immune evasion, Nat. Commun. 13 (1) (2022) 6308, https://doi.org/10.1038/s41467-022-34064-4.

[9] D. Guo, Y. Tong, X. Jiang, Y. Meng, H. Jiang, L. Du, Q. Wu, S. Li, S. Luo, M. Li, et al., Aerobic glycolysis promotes tumor immune evasion by hexokinase2-mediated phosphorylation of IκBα, Cell Metabol. 34 (9) (2022) 1312–1324.e1316, https://doi.org/10.1016/j.cmet.2022.08.002.

[10] C.A. Borrebaeck, Precision diagnostics: moving towards protein biomarker signatures of clinical utility in cancer, Nat. Rev. Cancer 17 (3) (2017) 199–204, https://doi.org/10.1038/nrc.2016.153.

[11] C. Huang, L. Chen, S.R. Savage, R.V. Eguez, Y. Dou, Y. Li, F. da Veiga Leprevost, E.J. Jaehnig, J.T. Lei, B. Wen, et al., Proteogenomic insights into the biology and treatment of HPV-negative head and neck squamous cell carcinoma, Cancer Cell 39 (3) (2021) 361–379.e316, https://doi.org/10.1016/j.ccell.2020.12.007.

[12] J.R. Whiteaker, G.N. Halusa, A.N. Hoofnagle, V. Sharma, B. MacLean, P. Yan, J.A. Wrobel, J. Kennedy, D.R. Mani, L.J. Zimmerman, et al., CPTAC Assay Portal: a repository of targeted proteomic assays, Nat. Methods 11 (7) (2014) 703–704, https://doi.org/10.1038/nmeth.3002.

[13] M.E. Ritchie, B. Phipson, D. Wu, Y. Hu, C.W. Law, W. Shi, G.K. Smyth, Limma powers differential expression analyses for RNA-sequencing and microarray studies, Nucleic Acids Res. 43 (7) (2015) e47, https://doi.org/10.1093/nar/gkv007.

[14] T. Wu, E. Hu, S. Xu, M. Chen, P. Guo, Z. Dai, T. Feng, L. Zhou, W. Tang, L. Zhan, et al., clusterProfiler 4.0: a universal enrichment tool for interpreting omics data, Innovation 2 (3) (2021) 100141, https://doi.org/10.1016/j.xinn.2021.100141.

[15] W. Shen, Z. Song, X. Zhong, M. Huang, D. Shen, P. Gao, X. Qian, M. Wang, X. He, T. Wang, S. Li, X. Song, Sangerbox: a comprehensive, interaction-friendly clinical bioinformatics analysis platform, Imeta 1 (3) (2022 Jul 8) e36, https://doi.org/10.1002/imt2.36. PMID: 38868713; PMCID: PMC10989974.

[16] C. von Mering, M. Huynen, D. Jaeggi, S. Schmidt, P. Bork, B. Snel, STRING: a database of predicted functional associations between proteins, Nucleic Acids Res. 31 (1) (2003) 258–261, https://doi.org/10.1093/nar/gkg034.

[17] E.Y. Chen, C.M. Tan, Y. Kou, Q. Duan, Z. Wang, G.V. Meirelles, N.R. Clark, A. Ma'ayan, Enrichr: interactive and collaborative HTML5 gene list enrichment analysis tool, BMC Bioinf. 14 (2013 Apr 15) 128, https://doi.org/10.1186/1471-2105-14-128. PMID: 23586463; PMCID: PMC3637064.

[18] N. Simon, J. Friedman, T. Hastie, R. Tibshirani, Regularization paths for cox's proportional hazards model via coordinate descent, J. Stat. Software 39 (5) (2011 Mar) 1–13, https://doi.org/10.18637/jss.v039.i05. PMID: 27065756; PMCID: PMC4824408.

[19] S. Xu, H. Fu, S. Weng, X. Gu, J. Li, Derivation and comprehensive analysis of ageing-related genes in intervertebral disc degeneration for prediction and immunology, Mech. Ageing Dev. 211 (2023) 111794, https://doi.org/10.1016/j.mad.2023.111794.

[20] D.A. Barbie, P. Tamayo, J.S. Boehm, S.Y. Kim, S.E. Moody, I.F. Dunn, A.C. Schinzel, P. Sandy, E. Meylan, C. Scholl, et al., Systematic RNA interference reveals that oncogenic KRAS-driven cancers require TBK1, Nature 462 (7269) (2009) 108–112, https://doi.org/10.1038/nature08460.

[21] B. Zhang, Q. Wu, B. Li, D. Wang, L. Wang, Y.L. Zhou, m(6)A regulator-mediated methylation modification patterns and tumor microenvironment infiltration characterization in gastric cancer, Mol. Cancer 19 (1) (2020) 53, https://doi.org/10.1186/s12943-020-01170-0.

[22] K. Yoshihara, M. Shahmoradgoli, E. Martínez, R. Vegesna, H. Kim, W. Torres-Garcia, V. Treviño, H. Shen, P.W. Laird, D.A. Levine, et al., Inferring tumour purity and stromal and immune cell admixture from expression data, Nat. Commun. 4 (2013) 2612, https://doi.org/10.1038/ncomms3612.

[23] B. Lin, J. Xu, D.G. Feng, F. Wang, J.X. Wang, H. Zhao, DUSP14 knockout accelerates cardiac ischemia reperfusion (IR) injury through activating NF-κB and MAPKs signaling pathways modulated by ROS generation, Biochem. Biophys. Res. Commun. 501 (1) (2018) 24–32, https://doi.org/10.1016/j.bbrc.2018.04.101.

[24] D.J. Clark, S.M. Dhanasekaran, F. Petralia, J. Pan, X. Song, Y. Hu, F. da Veiga Leprevost, B. Reva, T.M. Lih, H.Y. Chang, et al., Integrated proteogenomic characterization of clear cell renal cell carcinoma, Cell 179 (4) (2019) 964–983.e931, https://doi.org/10.1016/j.cell.2019.10.007.

[25] L. Galluzzi, J. Humeau, A. Buqué, L. Zitvogel, G. Kroemer, Immunostimulation with chemotherapy in the era of immune checkpoint inhibitors, Nat. Rev. Clin. Oncol. 17 (12) (2020) 725–741, https://doi.org/10.1038/s41571-020-0413-z.

[26] B. Chen, M.S. Khodadoust, C.L. Liu, A.M. Newman, A.A. Alizadeh, Profiling tumor infiltrating immune cells with CIBERSORT, Methods Mol. Biol. 1711 (2018) 243–259, https://doi.org/10.1007/978-1-4939-7493-1_12. PMID: 29344893; PMCID: PMC5895181.

[27] E. Becht, N.A. Giraldo, L. Lacroix, B. Buttard, N. Elarouci, F. Petitprez, J. Selves, P. Laurent-Puig, C. Sautès-Fridman, W.H. Fridman, A. de Reyniès, Estimating the population abundance of tissue-infiltrating immune and stromal cell populations using gene expression, Genome Biol. 17 (1) (2016 Oct 20) 218, https://doi.org/10.1186/s13059-016-1070-5. Erratum in: Genome Biol. 2016 Dec 1;17(1):249. doi: 10.1186/s13059-016-1113-y. PMID: 27765066; PMCID: PMC5073889.

[28] Y. You, Y. Shan, J. Chen, H. Yue, B. You, S. Shi, X. Li, X. Cao, Matrix metalloproteinase 13-containing exosomes promote nasopharyngeal carcinoma metastasis, Cancer Sci. 106 (12) (2015) 1669–1677, https://doi.org/10.1111/cas.12818.

[29] Q. Chu, H. Huang, T. Huang, L. Cao, L. Peng, S. Shi, L. Zheng, L. Xu, S. Zhang, J. Huang, et al., Extracellular serglycin upregulates the CD44 receptor in an autocrine manner to maintain self-renewal in nasopharyngeal carcinoma cells by reciprocally activating the MAPK/β-catenin axis, Cell Death Dis. 7 (11) (2016) e2456, https://doi.org/10.1038/cddis.2016.287.

[30] Q. Zhu, A.L. Zhong, H. Hu, J.J. Zhao, D.S. Weng, Y. Tang, Q.Z. Pan, Z.Q. Zhou, M.J. Song, J.Y. Yang, et al., Correction: acylglycerol kinase promotes tumour growth and metastasis via activating the PI3K/AKT/GSK3β signalling pathway in renal cell carcinoma, J. Hematol. Oncol. 16 (1) (2023) 110, https://doi.org/10.1186/s13045-023-01505-6.

[31] M. Zhao, R. Luo, Y. Liu, L. Gao, Z. Fu, Q. Fu, X. Luo, Y. Chen, X. Deng, Z. Liang, et al., miR-3188 regulates nasopharyngeal carcinoma proliferation and chemosensitivity through a FOXO1-modulated positive feedback loop with mTOR-p-PI3K/AKT-c-JUN, Nat. Commun. 7 (2016) 11309, https://doi.org/10.1038/ncomms11309.

[32] J. Zhang, L. Jia, T. Liu, Y.L. Yip, W.C. Tang, W. Lin, W. Deng, K.W. Lo, C. You, M.L. Lung, et al., mTORC2-mediated PDHE1α nuclear translocation links EBV-LMP1 reprogrammed glucose metabolism to cancer metastasis in nasopharyngeal carcinoma, Oncogene 38 (24) (2019) 4669–4684, https://doi.org/10.1038/s41388-019-0749-y.
[33] S. Luangdilok, C. Box, L. Patterson, W. Court, K. Harrington, L. Pitkin, P. Rhŷs-Evans, O.c. P, S. Eccles, Syk tyrosine kinase is linked to cell motility and progression in squamous cell carcinomas of the head and neck, Cancer Res. 67 (16) (2007) 7907–7916, https://doi.org/10.1158/0008-5472.Can-07-0331.
[34] M. Tang, X. Dong, L. Xiao, Z. Tan, X. Luo, L. Yang, W. Li, F. Shi, Y. Li, L. Zhao, et al., CPT1A-mediated fatty acid oxidation promotes cell proliferation via nucleoside metabolism in nasopharyngeal carcinoma, Cell Death Dis. 13 (4) (2022) 331, https://doi.org/10.1038/s41419-022-04730-y.
[35] Z. Tan, L. Xiao, M. Tang, F. Bai, J. Li, L. Li, F. Shi, N. Li, Y. Li, Q. Du, et al., Targeting CPT1A-mediated fatty acid oxidation sensitizes nasopharyngeal carcinoma to radiation therapy, Theranostics 8 (9) (2018) 2329–2347, https://doi.org/10.7150/thno.21451.
[36] M. Soltani, Y. Zhao, Z. Xia, M. Ganjalikhani Hakemi, A.V. Bazhin, The importance of cellular metabolic pathways in pathogenesis and selective treatments of hematological malignancies, Front. Oncol. 11 (2021) 767026, https://doi.org/10.3389/fonc.2021.767026.
[37] X. Wang, Z. Xiang, G.S. Tsao, W. Tu, Exosomes derived from nasopharyngeal carcinoma cells induce IL-6 production from macrophages to promote tumorigenesis, Cell. Mol. Immunol. 18 (2) (2021) 501–503, https://doi.org/10.1038/s41423-020-0420-0.
[38] L. Wei, X. Zhang, J. Wang, Q. Ye, X. Zheng, Q. Peng, Y. Zheng, P. Liu, X. Zhang, Z. Li, et al., Lactoferrin deficiency induces a pro-metastatic tumor microenvironment through recruiting myeloid-derived suppressor cells in mice, Oncogene 39 (1) (2020) 122–135, https://doi.org/10.1038/s41388-019-0970-8.
[39] R. Hopkins, W. Xiang, D. Marlier, V.B. Au, Q. Ching, L.X. Wu, R. Guan, B. Lee, W.K. Chia, W.W. Wang, et al., Monocytic myeloid-derived suppressor cells underpin resistance to adoptive T cell therapy in nasopharyngeal carcinoma, Mol. Ther. 29 (2) (2021) 734–743, https://doi.org/10.1016/j.ymthe.2020.09.040.
[40] S. Huo, Y. Luo, R. Deng, X. Liu, J. Wang, L. Wang, B. Zhang, F. Wang, J. Lu, X. Li, EBV-EBNA1 constructs an immunosuppressive microenvironment for nasopharyngeal carcinoma by promoting the chemoattraction of Treg cells, J Immunother Cancer 8 (2) (2020), https://doi.org/10.1136/jitc-2020-001588.
[41] C.J. Caunt, S.M. Keyse, Dual-specificity MAP kinase phosphatases (MKPs): shaping the outcome of MAP kinase signalling, FEBS J. 280 (2) (2013) 489–504, https://doi.org/10.1111/j.1742-4658.2012.08716.x.
[42] Y. Wei, G. Wang, C. Wang, Y. Zhou, J. Zhang, K. Xu, Upregulation of DUSP14 affects proliferation, invasion and metastasis, potentially via epithelial-mesenchymal transition and is associated with poor prognosis in pancreatic cancer, Cancer Manag. Res. 12 (2020) 2097–2108, https://doi.org/10.2147/cmar.S240040.